

Diffusion-weighted imaging findings in Perthes disease with dynamic gadolinium-enhanced subtracted (DGS) MR correlation: a preliminary study

Laura Merlini · Christophe Combescure ·
Vincenzo De Rosa · Mehrak Anooshiravani ·
Sylviane Hanquinet

Received: 26 January 2009 / Revised: 24 September 2009 / Accepted: 26 September 2009 / Published online: 6 January 2010
© Springer-Verlag 2009

Abstract

Background Legg-Calvé-Perthes disease (LCP) is necrosis of the proximal femoral epiphysis of vascular origin. Clinical course and outcome in LCP disease varies considerably between different patients. Earlier prognostic criteria than those offered by conventional radiography are necessary to identify children who require prompt surgical treatment.

Objective To assess the significance of signal alteration on diffusion-weighted MR imaging (DWI MR) in LCP.

Materials and methods Twelve boys with unilateral LCP disease (Catterall grade 2 and 3), at the initial sclerotic stage and early fragmentation phase, underwent dynamic gadolinium-enhanced subtracted (DGS) and DWI MR. For DGS MR, the lateral pillar enhancement was recorded. For DWI imaging, we measured ADC values in the diseased and the unaffected epiphyses and metaphyses. Receiver operating characteristic curves were performed to analyze the performance of DWI in establishing agreement with the results of DGS MR, which is the gold standard for prognosis.

Results Femoral epiphysis increased diffusivity was observed in the affected hip in all cases. Increased metaphysis diffusivity in the affected side was observed in all cases with absent lateral pillar enhancement at DGS MR.

Conclusion DWI seems to be a noninvasive means of distinguishing between Perthes disease with favourable and unfavourable prognosis.

Keywords Legg-Calvé-Perthes disease · MR · Diffusion · Child

Introduction

Legg-Calvé-Perthes disease (LCP) is necrosis of the proximal femoral epiphysis of vascular origin [1, 2]. Clinical course and outcome in LCP disease varies considerably between different patients. Earlier prognostic criteria than those offered by conventional radiography are necessary to identify children who require prompt surgical treatment [3].

In the past, pinhole scintigraphy was considered the gold standard for prognosis of LCP due to its ability to assess the revascularization pattern [4, 5]. There are two characteristic revascularization patterns on scintigraphy. With type A ('alright'), which carries a good prognosis, there is activity along the lateral column. With type B ('bad'), which has a poor prognosis, scintigraphy reveals a pattern of base filling or 'mushrooming'. A third process (stage C) can occur when stage A is transformed to stage B [6].

Many studies have assessed the very high reproducibility of a scintigraphic model on dynamic gadolinium-enhanced subtracted (DGS) MR allowing the use of the latter as the new gold standard in assessing prognosis in Perthes disease

L. Merlini (✉) · M. Anooshiravani · S. Hanquinet
Unit of Pediatric Radiology, Geneva University Hospital,
rue Willy-Donzé 6,
Geneva 1205, Switzerland
e-mail: laura.merlini@hcuge.ch

C. Combescure
Department of Biostatistics, University Hospital of Geneva,
Geneva, Switzerland

V. De Rosa
Clinic of Pediatric Orthopedics, University Hospital of Geneva,
Geneva, Switzerland

[4, 7, 8]. The early appearance of lateral pillar enhancement is indicative of uncomplicated revascularisation of the femoral head and, thus, of good prognosis. The second mechanism represents a slower rate of neovascularisation and healing and is depicted by DGS MR as absence of lateral pillar enhancement. Enhancement of the metaphyseal region is reported in the literature as having a high positive predictive value (92%) for a poor prognosis [4, 7, 8].

Apart from the absence of radiation, MR provides optimal anatomical detail compared to scintigraphy. The necessity of contrast utilization however has recently raised concern about collateral and rare effects such as nephrogenic systemic fibrosis (NSF).

Preliminary experimental studies on surgically induced hip ischaemia in piglets have shown that diffusion-weighted MR (DWI) changes are a good marker of epiphyseal destruction [9, 10].

This is the first paper to evaluate the feasibility and value of DWI in LCP disease. In our study we compared DWI MR to DGS MR in order to investigate if this noninvasive technique would be helpful in distinguishing between LCP disease with favourable and unfavourable prognosis, which may influence the choice of treatment modality.

The Institutional Ethic Board of the University Hospital of Geneva approved this study.

Materials and methods

Patients

Twelve boys aged between 5 and 12 years with a diagnosis of Perthes disease made on plain films and/or on bone scintigraphy were recruited during the period January 2006 to May 2008 (Table 1). All children were initially seen by a senior paediatric orthopaedic doctor (V.D.R.; 14 years of experience). MR imaging was performed 1–6 months after the first onset of symptoms of LCP disease. Inclusion criteria were: Catterall classification on radiography stage 2 ($n=8$) or 3 ($n=4$) [11]; unilateral LCP in order to allow comparison with the unaffected contralateral side as control group; and age at presentation >5 years.

Imaging

MR was performed on a 1.5-T unit (Avanto, Siemens, Germany) using a six-element body-array coil positioned on the anterior ventral part of the child combined with six elements of the spine coil. Geometric imaging parameters common to all morphological sequences were: FOV 270×270 mm; slice thickness 5 mm with a 1-mm gap; 367×448 matrix; 1–3 averages; voxel size

Table 1 Results of MR for the pathological hip (DGS MR: + lateral pillar enhancement is present, – lateral pillar enhancement is absent. DWI femoral head: + ADC value $>0.860 \times 10^{-3} \text{ mm}^2/\text{s}$ (cut-off for diagnosis), – ADC value $<0.860 \times 10^{-3} \text{ mm}^2/\text{s}$ (cut-off for diagnosis). DWI metaphysis: + ADC value $>1.042 \times 10^{-3} \text{ mm}^2/\text{s}$ (cut-off for prognosis), – ADC value $<1.042 \times 10^{-3} \text{ mm}^2/\text{s}$. Catterall classification in conventional radiography)

Patient	Age (years)	DGS MR	DWI epiphysis	DWI metaphysis	Catterall
1	10.5	–	+	+	3
2	7.8	–	+	+	3
3	8.4	+	+	–	3
4	6.3	+	+	+	2
5	6.0	+	+	–	2
6	6.0	–	+	+	2
7	7.3	–	+	+	2
8	5.33	–	+	+	2
9	12.0	+	+	–	2
10	5.9	–	+	+	3
11	7.0	–	+	+	2
12	6.1	+	+	–	2

$0.8 \times 0.7 \times 5 \text{ mm}$. The following sequences were obtained: T1-weighted (T1-W) coronal spin-echo (SE) (TR 500 ms; TE 20 ms) and both proton-density (PD) and T2-weighted (T2-W) coronal turbo SE (TSE), (TR 2,000 ms; TE 80 ms) (T2-W); TE 20 ms (PD). Dynamic T1-W SE sequence (TR 200 ms; TE 20 ms; acquisition time 1 min) was first obtained at five levels, all including the femoral head, in the coronal plane. A bolus of 0.1 mmol/kg gadolinium tetra-azacyclo-dodecane-tetraacetic acid (DOTA; Dotarem, Guerbet, Aulnay, France) was injected manually in <15 s, followed by a 10-ml saline flush. Images were acquired at the same five levels as before, every minute for 5 min after the beginning of the injection. The 1-, 2-, 3-, 4- and 5-min contrast-enhanced images were then subtracted from the precontrast images, using the subtraction function available as standard software on our console.

DWI sequences were performed before contrast medium injection and consisted of 20 coronal slices (at least 10 through the femoral head), acquired using an SE-based EPI sequence. Diffusion weighting was obtained using bipolar gradient preparation and three b- values: 50, 400, and 800 s/mm^2 . Diffusion gradients were applied concurrently in read, phase and slice directions in order to offer three orthogonal direction diffusion weightings sequentially. MR parameter utilized included: slice thickness 4 mm; phase-encoding direction right to left; EPI factor 156; matrix size 156×192; FOV 267×328 mm; voxel size 1.7×1.7×4 mm; TR 500 ms; TE 76 ms; bandwidth 1,736 Hz/pixel; the sequence was implemented with parallel imaging (grappa factor=2) and four averages. Apparent diffusion coefficient

(ADC) maps were calculated in line with ADC values in each pixel. They were calculated as a log linear fit of all measured diffusion values times. ADC maps display all ADC above a threshold value chosen equal to the noise mean value.

No automatic coregistration between DGS and DWI was performed; visual image matching was used.

Image analysis

On DGS MR, enhancement in the lateral pillar was used as a sign of good prognosis. Enhancement intensity of the ischaemic femoral head lateral pillar was qualitatively compared to the contralateral side on subtraction images, using slices with the most intense enhancement. We did not measure enhancement ratios. Two senior paediatric radiologists with 6 and 15 years of experience (L.M. and M.A., respectively) scored the images by consensus. There were no disagreements between the two readers. The enhancement intensity of the epiphysis was compared with that of the contralateral hip and classified as increased (+) with a good prognosis, or not increased (–) with a bad prognosis (Fig. 1). Enhancement intensity of the metaphysis immediately adjacent to the physis (metaphyseal spongiosa) was compared with the same region on the control hip and classified according to the same criteria (Fig. 3). The results are shown in Table 1.

On DWI, the same radiologists assessed the b400 DW images blindly and reached a consensus for image quality with a two-point scale (1=background noise and distortion artefacts due to susceptibility or eddy currents; 2=minor background noise and no distortion of the image). This made it easier to assess certain features: the bone structure; presence or absence of hyperintensity in the epiphysis compared to the same region in the control hip; and presence or absence of hyperintensity in the metaphysis adjacent to the physis compared to the same region in the control hip.

Measurements of diffusivity on ADC maps were performed once by two radiologists (L.M. and M.A.) independently and blinded to all other results. ADC was symmetrically measured on automatically generated ADC

maps both for the ischaemic and contralateral femoral epiphysis by positioning the largest possible user-defined region of interest (ROI), on the whole head, regardless of the signal intensity on T1-W, T2-W or DWI sequences, carefully excluding cartilage and fluid. The measurable area was 43 to 98 mm². For each child, ADC value on the epiphysis was a mean of measurement on at least five slices. The ADC value was also symmetrically measured in the femoral metaphysis adjacent to the physis (metaphyseal spongiosa) with the same procedure on both the pathological and contralateral side.

Statistical methods

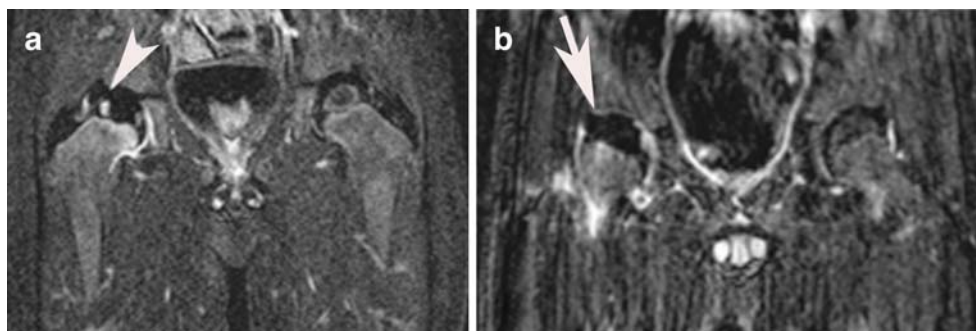
The quantitative variables were described by median values and range and the qualitative variables were described by figures and percentages.

Variable ADC values in epiphysis and metaphysis were compared between control and pathological sides by using Mann-Whitney tests and the ability of each variable to predict the diagnosis (pathological or control side) was assessed.

In the analysis of the prognostic performance of femoral epiphysis and metaphysis ADC values, DGS MR was considered the gold standard. The ability of each variable to predict the results of DGS MR was represented by a receiver operating characteristic (ROC) curve and the corresponding area under the curve (AUC). The ROC curves and AUC were assessed and compared by a non-parametric method [12]. Ninety-five-percent confidence intervals of the AUC were given. The optimal cut-offs were determined by minimizing the number of misclassified patients (number of false positives plus number of false negatives). When the ADC value was above the cut-off it was described as positive (+) and when it was below the cut-off it was described as negative (–). At the optimal cut-off, the sensitivities and specificities were calculated with the exact 95% confidence interval.

The inter-observer reproducibility of the ADC values was analyzed. The intraclass correlation coefficient was

Fig. 1 DGS MR. **a** A 6.1-year-old boy. An example of good enhancement of the lateral pillar (arrow). Children with this pattern were considered as having a good prognosis. **b** A 7.3-year-old boy shows lack of enhancement of the lateral pillar (arrow). Children with this pattern were considered as having bad prognosis



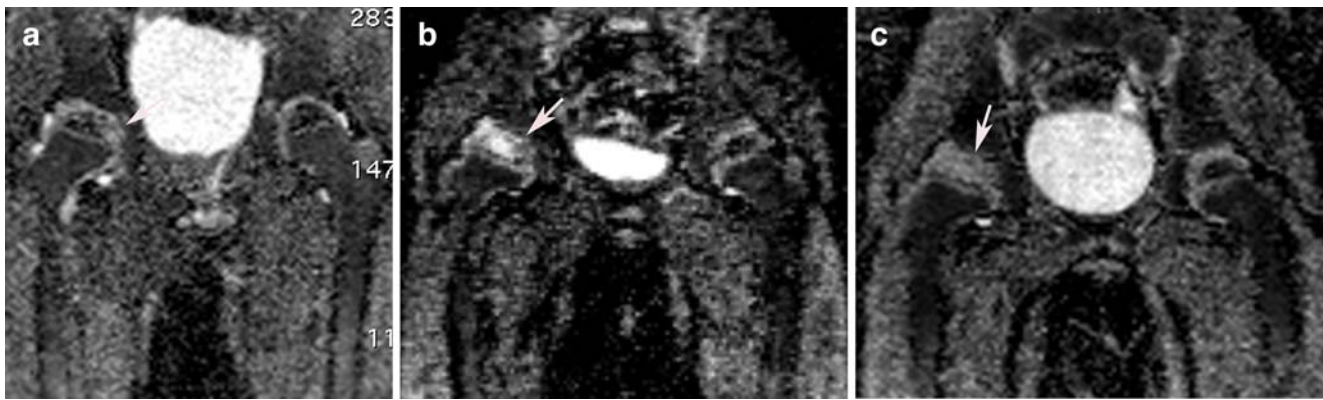


Fig. 2 b400 DWI average map shows different patterns of signal alteration in the pathological femoral epiphysis. **a** A 6.1-year-old boy. Hyperintensity is limited to the internal pillar (*arrow*). **b** A 6-year-old boy. The central part of the head is heavily hyperintense (*arrow*). **c** A

6.3-year-old boy. The whole epiphysis (*arrow*) is homogeneously slightly hyperintense. We did not classify the different patterns and did not correlate each pattern to results of DGS MR, because of the important dispersion of our data due to the small sample

assessed for ADC values in the epiphysis and metaphysis [13]. The precision was also assessed from a Bland and Altman graph (figures not shown).

Comparisons were considered significant if $P < 0.05$. We used the software S-Plus 2000 and SPSS 15.0.1 to perform the statistical analyses.

Results

Conventional radiology

Radiographically, eight children were classified as grade 2 and four as grade 3 according to the Catterall classification. Metaphyseal involvement was not depicted in any of the children (Table 1). No signs of head at risk (lateral subluxation, metaphyseal cystic changes, lateral calcification, Gage sign and horizontal growth plate) were present. MR was performed in five cases in the initial stage of the disease and in eight in the early

fragmentation stage. During follow-up, six children underwent surgery.

DGS MR

In the 12 normal hips, gadolinium injection resulted in early rapid (0–2 min) and intense enhancement of the femoral head. In pathological hips, lateral pillar enhancement in DGS MR was shown in 5 of the 12 who were considered positive (good prognosis) (Fig. 1). In seven children, the lateral pillar did not enhance (Fig. 1) and they were considered negative (bad prognosis) (Table 1). No cases in our study were in the pre-radiological phase: this observation can be of indeterminate prognosis due to the fact that recanalisation has simply not yet started.

Contrast enhancement of the metaphyseal region on DGS MR was present in five of seven children without contrast enhancement of the lateral pillar and was absent in all children with contrast enhancement of the lateral pillar.

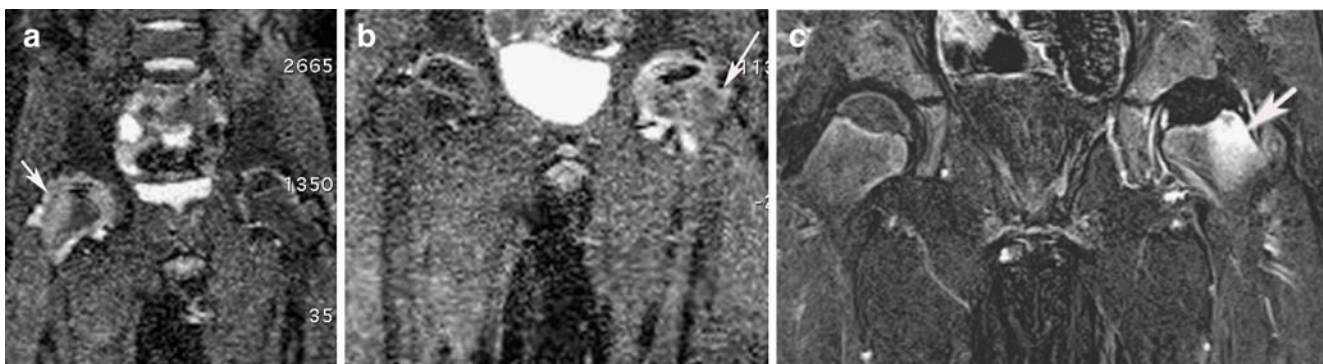


Fig. 3 Increased signal in the metaphyseal region (*arrows*) on DWI (**a**, **b**) and DGS MR (**c**)

Table 2 Summary table of ADC value ($\times 10^{-3}$ mm²/s). Comparison of ADC values of the metaphysis between control and pathological sides. $P=0.01$ between control and pathological sides for the epiphysis. Comparison of the ratio of ADC values pathological/control sides between metaphysis and epiphysis: $P<0.01$ (Mann-Whitney)

	Pathological epiphyses <i>n</i> =12	Control epiphyses <i>n</i> =12	Pathological metaphyses <i>n</i> =12	Control metaphyses <i>n</i> =12	Ratio of epiphyses <i>n</i> =12	Ratio of metaphyses <i>n</i> =12
Median	1.323	0.539	1.136	0.592	2.6	1.7
Minimum	0.908	0.355	0.486	0.420	1.3	0.9
Maximum	1.713	0.853	1.558	0.832	6.2	2.7
Average	1.298	0.514	1.018	0.599	3.0	1.7
	$P<0.01$		$P=0.01$		$P<0.01$	

DWI

Signal-to-noise ratio (SNR) was considered qualitatively as good (score 2) by both radiologists in all examinations (b400 DWI).

Within the epiphysis of the femoral head, increased signal intensity (SI) on b400 DWI was always observed with different patterns in all the pathological hips (Fig. 2).

In terms of assessment of the metaphysis, when compared to the contralateral hip, hyperintensity of the metaphysis was found in 8 of the 12 children (Fig. 3). Seven showed no contrast enhancement and one good contrast enhancement of the lateral pillar on DGS MR. Four children with no increased SI of the metaphysis showed good enhancement of the lateral pillar on DGS MR (Table 1).

We first studied the ability of ADC measurement (ADC maps) to distinguish between the pathological and control side separately in the femoral epiphysis and metaphysis. The intraclass correlation coefficient indicated excellent reproducibility of ADC values in both the epiphysis and metaphysis (>0.99 for both). The coefficient of variation for the epiphysis was 1.9% (median),

range 0.2–22.5%, and 1.4% (median), range 0.2–11.4%, in the metaphysis. The precision (from Bland and Altman method) was acceptable for both epiphysis and metaphysis, but better for the metaphysis [(-113; 72) and (-65; 44), respectively].

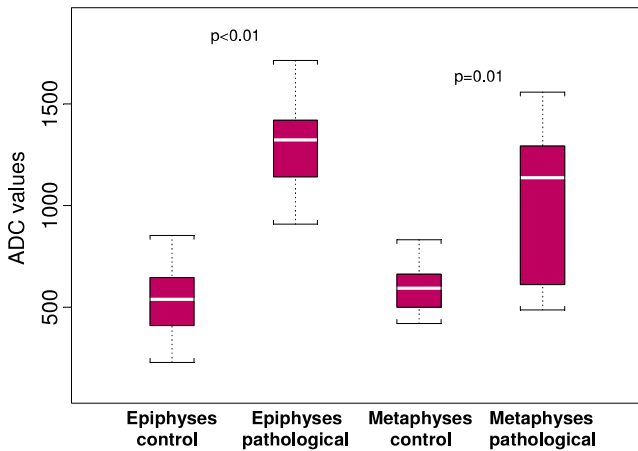
The Bland-Altman analysis revealed a mean difference between the two observers of 0.021×10^{-3} mm²/s for the epiphysis (with limits of agreement -0.113×10^{-3} mm²/s and 0.072×10^{-3} mm²/s) and of -0.011×10^{-3} mm²/s for the metaphysis (with limits of agreement -0.065×10^{-3} mm²/s and 0.044×10^{-3} mm²/s). The standard deviation between the pairs of measurements from the two observers divided by the average of the mean of each pair of results was 5.1% for the epiphysis and 3.4% for the metaphysis; the variability of the difference between the two readers was not relevant with regard to the mean ADC value.

ADC values of the femoral epiphysis and metaphysis were significantly higher for the pathological sides than for the control hips ($P<0.01$ and $P=0.01$, respectively; Mann-Whitney test). The median and range of ADC values are shown in Table 2 and 4. The ratios between pathological and control sides were also significantly higher for the ADC values in the epiphysis than

Table 3 Summary of well and misclassified sides/children at the selected cut-offs

		Diagnosis	
		Control sides (<i>n</i> =12)	Pathological sides (<i>n</i> =12)
ADC epiphysis	No	12	0
≥ 0.860	Yes	0	12
ADC metaphysis	No	12	4
≥ 1.000	Yes	0	8
		Prognosis	
		Group A (<i>n</i> =5 patients)	Group B (<i>n</i> =7 patients)
ADC epiphysis	No	3	1
≥ 1.193	Yes	2	6
ADC metaphysis	No	4	0
≥ 1.042	Yes	1	7

Table 4 Box plot of the ADC values representing the median, the interquartile interval and the range



in the metaphysis (neck) ($P < 0.01$; Mann-Whitney test) (Table 2).

In the epiphysis, a cut-off value of $0.86 \times 10^{-3} \text{ mm}^2/\text{s}$ correctly identified all 12 pathological sides (sensitivity=100.0%, $CI_{95\%}=[73.5-100.0]$) and all of the 12 control sides (specificity=100.0%, $CI_{95\%}=[73.5-100.0]$). The AUC was equal to 1.00.

In the metaphysis, a cut-off value of $1.042 \times 10^{-3} \text{ mm}^2/\text{s}$ (minimum misclassified cases) correctly identified 8 of the 12 pathological sides (sensitivity=66.7%, $CI_{95\%}=[34.9-90.1]$), and all of the 12 control sides (specificity=100%, $CI_{95\%}=[73.5-100.0]$). The misclassified sides (four false

negative) were all pathological sides (Table 3). AUC of ADC metaphysis was equal to 0.799 ($CI_{95\%}=[0.608-0.989]$).

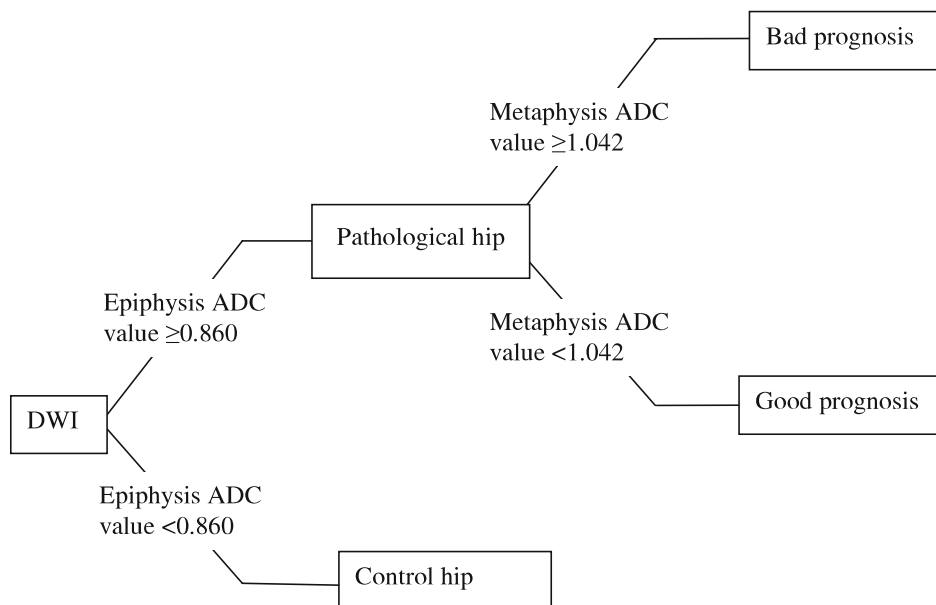
Secondly, we studied the ability of DWI to predict the result of DGS MR separately for the femoral epiphysis and metaphysis. In the epiphysis, the cut-off value of $1.193 \times 10^{-3} \text{ mm}^2/\text{s}$ (minimizing the number of misclassified sides) led to two false positives and one false negative (sensitivity=91.7%, $CI_{95\%}=[61.5-99.8]$; specificity=83.3%, $CI_{95\%}=[51.6-97.9]$). The AUC was equal to 0.686 ($CI_{95\%}=[0.366-1.000]$).

In the metaphysis (minimized number of misclassified sides), the cut-off value was $1.000 \times 10^{-3} \text{ mm}^2/\text{s}$, leading to one false positive and no false negatives (sensitivity=100.0%, $CI_{95\%}=[73.5-100.0]$; specificity=91.7%, $CI_{95\%}=[61.5-99.8]$). The AUC was equal to 0.800 ($CI_{95\%}=[0.449-1.000]$).

Discussion

Our study considers children with unilateral Perthes disease classified as Catterall grade 2 and 3, at the initial sclerotic stage and early fragmentation phase. The children were older than 5 years; younger children were excluded because this age group has a good prognosis and early prognostic signs are, therefore, of little value. Furthermore, the inhomogeneity of the epiphyseal femoral marrow in early childhood may cause difficulty in interpretation. In the first years of life the red haemopoietic marrow (cellular) has

Table 5 Graphical representation of the potential decision rule. (ADC units $\times 10^{-3} \text{ mm}^2/\text{s}$)



high ADC values and becomes progressively yellow marrow (fatty) with lower ADC values. ADC values for the normal paediatric femoral epiphysis at different ages has not yet been validated, but after 5 years it is presumed to be homogeneous [14, 15]. To overcome this problem we considered only unilateral Perthes disease, in order to compare ADC data of the affected side to the control hip in the same subject.

The DWI technique was of good quality (SNR), with good reproducibility and precision (intraclass correlation).

Increased diffusivity was demonstrated within ROIs drawn on ADC maps. b400 s/mm² DW images were used for positioning ADC ROIs: b400 was considered the best compromise between efficient diffusion weighting and image deterioration associated with diffusion weighting [16]. However, the increased SI visible on b400 DW sequence in the increased diffusivity areas is mainly due to T2 shine-through phenomenon (Fig. 2).

One option to overcome this problem in future studies would be to fuse b800 (showing only zones of signal change, but with poor anatomical definition) with T1-W precontrast-enhanced sequences, in order to obtain restricted-diffusion-zone imaging as well as anatomical definition. The development of DWI sequences with shorter TEs will also decrease susceptibility artefacts and increase SNR.

Increased SI is always observed in the pathological femoral epiphysis. The observation that ADC measurement in the epiphysis can easily distinguish between the pathological and control side (Table 3) is not clinically relevant at Catterall stages 2 and 3, as in our study. It would, however, be interesting to find a cut-off between pathological and control hips in the pre-radiological stage, supplanting the need for contrast-enhanced MR (Tables 4 and 5).

No particular ADC threshold value in the femoral capital epiphysis was found to correlate with presence or absence of lateral pillar enhancement on DGS MR. In fact, experimental studies in animals provide some evidence that DGS MR and DWI MR changes in the femoral epiphysis are expressions of two different processes with different time courses: perfusion abnormalities affect gadolinium enhancement whereas histological changes, such as cartilaginous islands within the bone and decreased fatty marrow, could increase diffusion [10]. For prognosis, on the basis of this observation, one can suggest comparing DGS MR to DWI with $b < 100$ s/mm² (b100 DWI is mostly influenced by perfusion phenomenon).

Alternatively, increased metaphyseal diffusivity (ADC maps) correlates well with absent lateral pillar enhancement on DGS MR, distinguishing between Perthes disease with favourable and unfavourable prognosis. Among the 12 children, only 1 was misclassified (1 false positive who later became a true positive as a type C in the scintigraphic classification).

Increased enhancement of the pathological metaphyseal region compared to the normal side on DGS MR was found in five of seven children with worse prognostic factors. In other words, DWI seems more sensitive to metabolic changes in the metaphysis than DGS MR. The pathological significance of this sign remains to be elucidated; animal models suggest that fibrovascular tissue has resorbed and replaced the metaphyseal bone and this tissue can be responsible for the increased ADC value [17].

ADC value measurements we report may not necessarily apply when performed on different machines [18]. Moreover, due to the limited number of enrolled children, the statistical power of our study is weak and a definitive cut-off cannot be reliably estimated. Reliable DWI maps in children are not yet available in the literature, and are probably difficult to obtain due to the patchy nature of bone marrow in childhood. However, in our study, based on ADC measurements, the suggested decision rule led only to one incorrect prognosis.

Future follow-up studies will allow correlation between clinical long-term results and prognostic assessment provided by imaging.

Conclusions

The preliminary results of our study in the field of DWI in Perthes disease are encouraging. DWI MR seems to be a noninvasive means of distinguishing between Perthes disease with favourable and unfavourable prognosis.

References

1. Wall EJ (1999) Legg-Calve-Perthes' disease. *Curr Opin Pediatr* 11:76–79
2. Salter RB (1980) Legg-Perthes disease: the scientific basis for the methods of treatment and their indications. *Clin Orthop Relat Res* 150:8–11
3. Wiig O, Terjesen T, Svenningsen S (2008) Prognostic factors and outcome of treatment in Perthes' disease: a prospective study of 368 patients with five-year follow-up. *J Bone Joint Surg Br* 90:1364–1371
4. Comte F, De Rosa V, Zekri H et al (2003) Confirmation of the early prognostic value of bone scanning and pinhole imaging of the hip in Legg-Calve-Perthes disease. *J Nucl Med* 44:1761–1766
5. Tsao AK, Dias LS, Conway JJ et al (1997) The prognostic value and significance of serial bone scintigraphy in Legg-Calve-Perthes disease. *J Pediatr Orthop* 17:230–239
6. Conway JJ (1993) A scintigraphic classification of Legg-Calve-Perthes disease. *Semin Nucl Med* 23:274–295
7. Ducou le Pointe H, Haddad S, Silberman B et al (1994) Legg-Perthes-Calve disease: staging by MRI using gadolinium. *Pediatr Radiol* 24:88–91
8. Lamer S, Dorgeret S, Khairouni A et al (2002) Femoral head vascularisation in Legg Calve-Perthes disease: comparison of

- dynamic gadolinium-enhanced subtraction MRI with bone scintigraphy. *Pediatr Radiol* 32:580–585
9. Jaramillo D, Connolly SA, Vajapeyam S et al (2003) Normal and ischemic epiphysis of the femur: diffusion MR imaging study in piglets. *Radiology* 227:825–832
 10. Menezes NM, Connolly SA, Shapiro F et al (2007) Early ischemia in growing piglet skeleton: MR diffusion and perfusion imaging. *Radiology* 242:129–136
 11. Catterall A (1981) Legg-Calve-Perthes syndrome. *Clin Orthop Relat Res* 158:41–52
 12. Hanley JA, McNeil BJ (1983) A method of comparing the areas under receiver operating characteristic curves derived from the same cases. *Radiology* 148:839–843
 13. Lee J, Koh D, Ong CC (1989) Statistical evaluation of agreement between two methods for measuring a quantitative variable. *Comput Biol Med* 19:61–70
 14. Nonomura Y, Yasumoto M, Yoshimura R et al (2001) Relationship between bone marrow cellularity and apparent diffusion coefficient. *J Magn Reson Imaging* 13:757–760
 15. MacKenzie JD, Gonzalez L, Hernandez A et al (2007) Diffusion-weighted and diffusion tensor imaging for pediatric musculoskeletal disorders. *Pediatr Radiol* 37:781–788
 16. Herneth AM, Ringl H, Memarsadeghi M et al (2007) Diffusion weighted imaging in osteoradiology. *Top Magn Reson Imaging* 18:203–212
 17. Kim HK, Skelton DN, Quigley EJ (2004) Pathogenesis of metaphyseal radiolucent changes following ischemic necrosis of the capital femoral epiphysis in immature pigs. A preliminary report. *J Bone Joint Surg Am* 86-A:129–135
 18. Oner AY, Aggunlu L, Akpek S et al (2007) Diffusion-weighted imaging of the appendicular skeleton with a non-Carr-Purcell-Meiboom-Gill single-shot fast spin-echo sequence. *AJR* 189:1494–1501